Fuel, Volume 273, August 2020, Article number 117614
DOI: 10.1016/j.fuel.2020.117614

Desulfurization using limestone during sludge incineration in a fluidized bed furnace: Increased risk of particulate matter and heavy metal emissions

Jianrui Zha [a,b], Yaji Huang [*,a], Peter T. Clough [b], Lu Dong [a], Ligang Xu [a], Lingqin Liu [a], Zhicheng Zhu [a], Mengzhu Yu [a]

[a] Key Laboratory of Energy Thermal Conversion and Control of Ministry of Education, School of Energy and Environment, Southeast University, Nanjing 210096, China

[b] Energy and Power Theme, Cranfield University, Bedford MK43 0AL, United Kingdom

Abstract: Incineration of sludge can be an effective method to minimise waste whilst producing useful heat. However, incineration can cause secondary pollution issues due to the emission of SO_2, therefore a set of experiments of sludge incineration in a bubble bed furnace were conducted with limestone addition to study desulfurization of sludge incineration flue gas. As expected, over 93% emission of SO_2 was reduced with limestone addition, and that of CO and NO_x were increased and decreased respectively when the fuel feeding rate raised. The distribution of fly ash was also increased by raising the fuel feeding rate due to increasing fragmentation of the ash. However, distributions of $PM_{2.5}$ and heavy metals in submicron particles have dramatically increased with limestone desulfurization. The mechanism was revealed by SEM and EDS statistical analysis, indicating that the reaction between aluminosilicate and calcium made particles agglomerate and eutectic mixtures form, these larger ash particles were found to divide between collection as cyclone ash and fragmentation into finer particles that bypassed the cyclone. Those fine particles provided more surface area for heavy metal condensation. Furthermore, it was found that the reaction mechanism for semi-volatile metals involved them being released from the sludge and forming PM_1 particles due to the vaporization-condensation mechanism, leading to higher emission of PM_1 and distribution of heavy metals in PM_1. Thus, it should be considered that there may actually be higher emission risks of PM and heavy metal emissions when aiming to desulfurize a flue gas using Ca-based minerals in certain circumstances.

Key words: Sludge incineration; Fluidized bed; Limestone desulfurization; Particulate matter; Heavy metals.

treatment. Disposal of sludge by application to soil or in the sea can cause environmental issues, since it contains abundant quantities of pathogens, poorly biodegraded organics as well as heavy metals. Thermal treatment, including combustion, gasification and pyrolysis, can thoroughly destroy the organics and pathogens in the sludge [1] . Fluidized beds are highly suited for incineration of dried granular sludge due to their higher combustion efficiency and heat and mass transfer than grate furnace, as well as more fuel flexibility than pulverised coal furnace. However, due to the nature of their operation, emissions of gaseous and aerated pollutants (SO_2, CO, NO_x, heavy metals, and dust) need to be effectively controlled [2] [3] .

Particulate matter (PM) is one of the main pollutants from solid fuel combustion. Coarse particles are mostly generated from the inorganic minerals by fragmentation and agglomeration, which can be captured by conventional bag filters or electrostatic precipitators [4] . Produced by coagulation and condensation, fine particles are often defined as submicron particles, which are more challenging to capture in conventional emission control systems and can be emitted to the atmosphere [5] [6] . In addition, those fine particles can contain many kinds of hazardous trace elements and can be inhaled into human lungs and be harmful to human health. Governments, internationally, have established plenty of laws and regulations to restrict the PM emission from combustion. In recent years, another formation mechanism for PM at the size of ~1-2.5 μm, this particle size range was identified as central mode, was found which was formed by the heterogeneous condensation or reaction of vaporized species on the surfaces of fine ash particles [7] , this mechanism differs from the formation of more conventional flue gas particulates. As the compositions and reactions of these minerals determine the PM formation and distribution, co-combustion or mineral addition can affect PM emissions [8-10].

Emissions of heavy metals is one of major problems in waste incineration processes, because they cannot be eliminated by altering combustion conditions. Alkali metals and some heavy metals such as lead, cadmium, zinc and copper which are named as semi-volatile metals and are likely enriched in fine ash [11] . Additionally, the

sludge ash could be classed as a hazardous material where concentrations of leachable heavy metals are too high. To control their emission, it is very important to understand the mechanisms that determine the behaviour of heavy metals. Temperature is a significant influencing factor on the partitioning of heavy metals because it decides when the phase changes and how fast the reactions happen. Moisture, sulphur and chlorine can also affect the behaviour of heavy metals by means of changing their volatility [12-14]. Some silicate minerals have been demonstrated to adsorb heavy metals at high temperatures, making a stable speciation and provides a route to form larger capturable particles [15-17].

SO_2 is also a gaseous pollutant from sludge incineration, whose removal methods include wet or dry flue gas desulfurization (W/D FGD), as well as in-furnace desulfurization by addition of calcium-based materials such as limestone. While WFGD is the most popular desulfurization technology, in-furnace desulfurization is preferred for fluidized beds as is much cheaper and convenient and has been successfully applied in the combustion industry. In addition, SO_2 is a known reactant for forming PM_1, thus some research has used Ca-based minerals to reduce the emission of submicron particles by absorbing SO_2 [18] .

Ca-based minerals also have been shown to have the potential for capturing heavy metals within a furnace. Zheng et al., modified limestone with K_2CO_3 and $Al_2(SO_4)_3$ to absorb heavy metals during wood sawdust combustion in a CO_2/O_2 atmosphere [19] . Wang et al., also found CaO could decrease the release of Pb [20] . However, some studies reached different conclusions, including Folgueras et al., who investigated the effect of inorganic matter on trace element behaviour during combustion of coal-sewage sludge blends. They found that as the ratio of Ca:Si in fuel increased lead and cadmium tended to be released from solid phase [21] . Lucie et al., reported a negative association of concentrations in ash yield between some trace elements and calcium during coal combustion, the reason of which was explained by the “dilution effect” of calcium [22] . Thus, calcium has a conflicting background towards heavy metal emissions and whether the effect on those elements

is retention or release depends on many conditions [14] . In general, it can be noted that when the ash yield in the fuel is low, the heavy metals tend to be adsorbed by calcium-based minerals, but if the inorganic matter in the fuel can react with calcium, the behaviour of heavy metals become complicated [14] .

Our previous paper investigated the effect of calcium on the heavy metal release during sludge incineration in a horizontal tube furnace, where the mineral reaction between calcium and aluminosilicate changed the retention rate of the heavy metals [23] . Obviously, the experiment on a horizontal tube furnace could indicate a mechanism for heavy metal behaviours but some factors during the real industrial combustion, such as particulate matter that is also significant for heavy metal emission, cannot be elucidates from those experiments. Since in-furnace desulfurization with limestone is a widely used method in fluidized bed incineration and its effect on the behaviour of heavy metals is debatable, this research looks to explore this topic in more detail and offer an analysis of the formation and transference mechanism for fine particulates and heavy metals. This paper aimed to further investigate the distributions of heavy metals during sludge incineration in a lab-scale fluidised bed furnace. The addition of limestone and the feeding rate of fuel were also accessed. Ash was sampled from all segments of the combustion process, of which fly ash was measured in different aerodynamic diameters in order to analyse the distribution of heavy metals.

2. Materials and methods

2.1 Materials

The sludge (25-800 μm in the form of granules, average particle size of 250 μm) was received pre-dried from a chemical fabric factory and its remaining moisture content was measured to be 6.2%. The composition analysis of the dried sludge is listed in Table 1. Volatile matter was 31.9%, while the ash content of the sludge is very high, at 58.2%. The analysis of the ash showed silicon and aluminium were the main components, and their

proportions were very close. Three heavy metals Pb, Cu and Zn were investigated in this paper and were found to have concentrations of 126, 103 and 742 mg·kg^{-1} respectively in the dried sludge.

Table 1. Composition of sludge (Dry basis)

Proximate analysis /%			Ultimate analysis / %					
Volatile matter	Ash	Fixed carbon	N	C	H	O	S	Cl
31.9	58.2	9.9	3.6	25.0	2.9	15.5	0.51	0.11
Heavy metal content / mg·kg^{-1}			Mineral content in ash / % (Expressed as oxide)					
Pb	Cu	Zn	SiO_2	Al_2O_3	CaO	P_2O_5	Fe_2O_3	TiO_2	K_2O
126	103	742	43.1	38.3	4.7	4.1	3.5	1.6	1.3

Within the fluidised bed, bauxite (mainly composed of Al_2O_3) with a particle size of 106-180 μm was used as bed material because it was less likely to cause agglomeration than sand (SiO_2), and limestone with a particle size of 200-400 μm for desulfurization (at a 2:1 mole ratio of Ca:S, about 3 wt% of sludge) was added in the sludge.

2.2 Experiment and analysis methods

The incineration tests were conducted in a lab-scale bubbling fluidised bed furnace (diameter 50 mm) as shown in Fig. 1. The height of dense phase zone is 400 mm from the bottom to screw feeder and the height of dilute phase zone is 600 mm from screw feeder to the top. The temperature in the furnace was controlled by two electric heaters and thermocouples for both zones. The inlet air flow for the furnace was 0.8 m^3/h constantly. Incineration conditions are listed in Table 2.

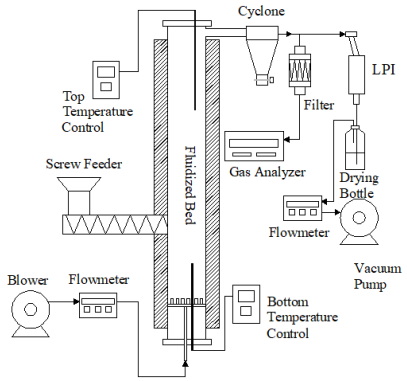

Fig. 1. System schematic of incineration furnace and sampling device

Table 2. Incineration conditions and naming

Naming of testing conditions		Feeding rate (g/h)	Fuel (wt%)	Dense phase zone temperature /℃	Dilute phase zone temperature /℃
SL	S1	267	100% Sludge	810	828
	S2	330	100% Sludge	822	831
CA	C1	269	97% Sludge + 3% Limestone	806	816
	C2	331	97% Sludge + 3% Limestone	814	825

Sampling of flue gas and ash was carried out when the combustion operating conditions were stable. The cyclone was designed to remove particulates bigger than 12.5μm, and unburned matter was measured by mass difference between the sample and its residue after being heated under 900 ℃. Gaseous product gas components (O_2, CO_2, NO_2, NO, SO_2, CO) in the flue gas were analysed by an infrared spectrometry gas analyser after an inline ash filter collected the fly ash. Some of the fly ash was diverted into a low-pressure-impactor (LPI) for determining the PM concentrations. LPI has eight stages ranging between 14.76-0.35 μm. The cyclone and flue gas pipelines were all trace heated (140 ℃) to prevent water condensing.

To determine heavy metal concentrations, the samples of sludge, bed ash, fly ash collected in the LPI were digested by HNO_3-HCl-HF-$HClO_4$, and were then measured using an atomic absorption spectrometry (AAS).

The surface morphology and composition of samples were analysed by a scanning electron microscopy (SEM) equipped with energy dispersed spectrum (EDS). Moreover, the crystal phase of sludge and cyclone ash was detected by X-ray diffraction (XRD) analysis.

The distributions of PM and heavy metals in the fly ash were normalized according to the total mass of input ash content.

2.3 Calculation of heavy metal enrichment in the ash

To assess the enrichment of heavy metal in a certain partition *n* of ash, the relative enrichment factor of RE_n was defined as:

$$RE_n = \frac{C_n}{C_{fuel}} \times \frac{(A_d)_{fuel}}{(A_d)_n} \quad (1)$$

Where, C_{fuel} and C_n are concentrations of heavy metal in the fuel and ash samples, respectively. $(A_d)_{fuel}$ and $(A_d)_n$ are percentages of ash content in the fuel and samples on a dry basis respectively. The factor $(A_d)_{fuel}$ is given in Table 1, and the factor $(A_d)_n$ is simplified as the residue rate of cyclone ash after heated at 900 °C. The heavy metals that tended to concentrate in the ash had a $RE_n > 1$, whereas those with a $RE_n < 1$ were dispersed in the samples.

3. Results and discussions

3.1 Flue gas analysis

Table 3. Flue gas analysis

Test	Excess air coefficient	SO_2 ($mg{\cdot}Nm^{-3}$, 11% O_2)	CO ($mg{\cdot}Nm^{-3}$, 11% O_2)	NO ($mg{\cdot}Nm^{-3}$, 11% O_2)	NO_2 ($mg{\cdot}Nm^{-3}$, 11% O_2)
S1	1.51	1978	1094	212	2

S2	1.31	1910	2089	163	1
C1	1.55	136	885	357	5
C2	1.32	127	1907	250	2

Flue gas analysis from combustion is shown in Table 3 where data were converted into standard conditions and at a baseline of 11% O_2 content. The addition of limestone decreased the SO_2 content dramatically from nearly 2000 to 130 mg/Nm^3 because of its desulfurization effect. The emission of CO seems to bear little relation to limestone addition but was influenced by the fuel feeding rate and the excess air coefficient. As for NO, both factors of limestone and excess air coefficient apparently impacted on its production. On the one hand, a reducing atmosphere in the furnace is known to reduce the formation of NO, but on the other hand, limestone was decomposed into CaO in the furnace which then catalysed the formation of NO [24] [25] . The concentration of NO_2 is very low due to the low furnace temperature. In brief, the limestone addition to the sludge presented a high efficiency for the removal of SO_2 but promoted the emissions of NO, and furthermore lowering the fuel feeding rate decreased the concentration of CO in the flue gas but increased the NO content.

3.2 Partition of ash and emission of PM

A mass balance was conducted by measuring the mass distributions of the ash streams (bed ash, cyclone ash, and fly ash) where had accumulated the ash for 2 hours in each sampling. Many factors should be considered for the calculation, such as ash partitioning and mass loss, as well as the unburned matters and limestone addition for desulfurization. The ash recovery rate was defined as the total amount of the inorganic components in the cyclone ash, fly ash and bed ash collected within a unit of time as a percentage of the inorganic content input from the fuel [26] . For each condition, the ash recovery rates were between 92-109%. The combustible matter in the cyclone ash varied from 1.4-2.7%, indicating the low unburned losses during the incineration tests. The

error values for ash balance were less than 7 % for each run.

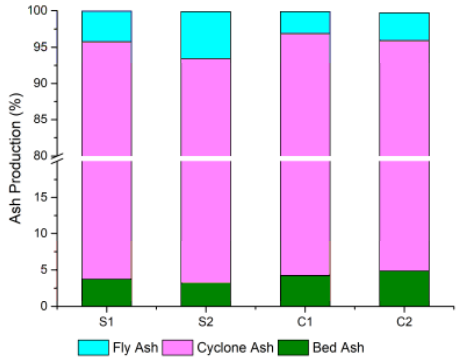

Fig. 2. Partitioning of the ash streams

The partitioning results of the ash streams is presented in Fig. 2. A higher fuel feeding rate increased the fly ash rates while limestone addition decreased its production yet. The limestone and sludge ash also reacted with bed material to form more bed ash, as the bed ash in the C1 test was detected to contain more calcium and silicon. Since the fine particles that passed through the cyclone often contain a greater content of heavy metals, it is preferable to target the reduction of fly ash production to minimise the disposal expense [27] .

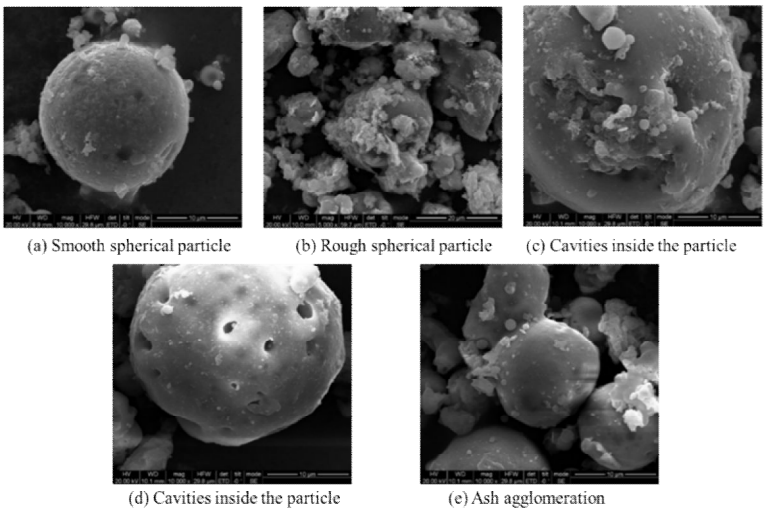

Fig. 3. Surface morphology of cyclone ash

Fig. 3 displays the micrographs of cyclone ash. In general, the surface morphologies of the cyclone ash can be approximated as smooth spheres with some finer particles adhered (Fig. 3a) or very rough with many particles layered (Fig. 3b). The spherical appearance indicated that the minerals of the fuel melted at the high bed

temperature.

Fig. 3c and Fig. 3d display the cavities of the particles, which appeared in larger number in samples from S1 and C1 tests. We hypothesize that these cavities were formed during the early combustion process of sludge, when the volatile matter from inside of the sludge particles was dramatically released at high temperature [28] . The higher fuel feeding rates for S2 and C2, likely made the furnace more fuel dense which resulted in a higher local temperature on the fuel particles as well as more inter-particle collisions. Because of this higher temperature, it is expected that the cavities were expanded more violently due to a faster reaction thus fragmenting into smaller pieces. This was the reason for a high fuel feeding rate leading to smaller particles forming and escaping through the cyclone.

Fig. 3e shows the two ash particles fused together into one larger particle, which were found more in CA tests (C1 and C2), indicating that the limestone addition stimulated the agglomeration and increased the diameter of ash, then decreased the amount of fly ash. This could possibly be due to the calcium in limestone partially fragmenting or interacting with aluminosilicates in the ash to form eutectic melts that adjoin between fine particles [29] .

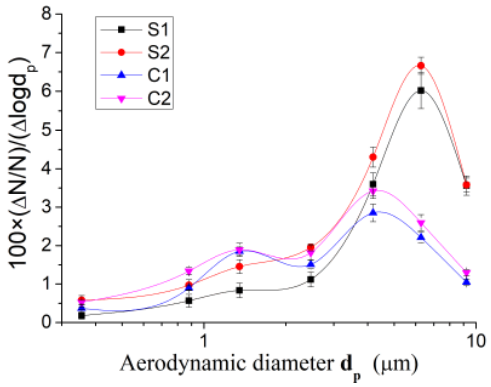

Fig. 4. PM distribution of the fly ash

PM distributions in fly ash are drawn in Fig. 4. The particle size distributions were very similar for the same composition curves of feedstock (S1-S2 and C1-C2), indicating that limestone addition likely played a role in

PM distribution as well. It can be also noted that the curves of S2 and C2 are higher than that of S1 and C1 respectively, likely because more fly ash was generated through fragment of bigger ash particles.

For the different conditions between SL tests (S1 and S2, without limestone addition) and CA tests (C1 and C2, with limestone addition), there is one sharp peak at about 7μm for each SL test, while for each CA condition test the distributions have a bimodal peak distribution at 1.3 and 4.3μm and the submicron particles were also increased. Many researchers have pointed out that the formation of ultra-fine particle (generally smaller than 0.5 μm) is as a result of heterogeneous and homogeneous coagulation of semi-volatile metals. In addition, some central mode particles can be in the size range of 0.5-2 μm [7] . As shown in Fig. 5, the reason why the distributions of PM_1 increased could be due to a higher vapor pressure of semi-volatile metals in the furnace to form ultra-fine particles, and the fragmentation of coarser particles to form central mode particles[17] .

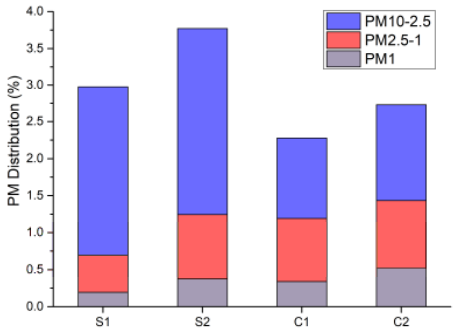

Fig. 5. Accumulations of PM distribution in the fly ash

The main peak shift from 7 to 4.3μm under desulfurization conditions can be explained as that coarser particles had more chance to collide and agglomerate together under calcium existing, and then left in cyclone ash, while smaller ash particles were less likely to collide with CaO (or limestone) and agglomerate. The reason for a greater amount of $PM_{2.5}$ observed in CA test conditions than those of SL test conditions can be considered to be caused by two probabilities. Firstly, limestone facilitated agglomeration into larger particles, which then broken up to form finer particles. Second, fine particulates from limestone fragmentation directly formed those finer particles. In order to confirm these possibilities, dozens of particles sampled from cyclone ash and fly ash

of S1 test (without limestone) and C1 test (with limestone), were analysed by EDS. Fig. 6 are bubble graphs for statistical analysis of the elements (Na+K) – Ca – (Si+Al) interactions by EDS (calculated excluding elemental carbon and oxygen). The size of bubbles represents the total mass fraction of Al and Si, and the coordinates of bubbles indicate the mass fractions of alkali metals and calcium.

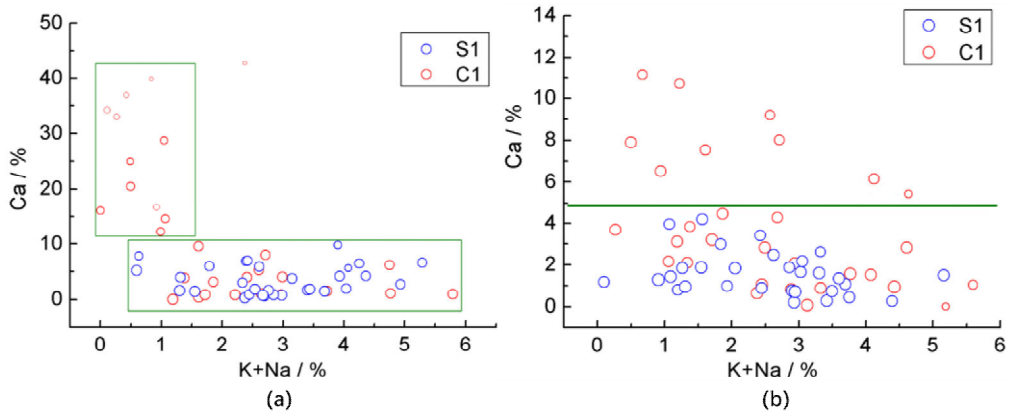

Fig. 6. Particle statistics of Ca - Na+K – Si+Al by EDS analysis of (a) Cyclone ash; (b) Fly ash.

In Fig. 6(a), most points of S1 and a part of C1 are uniformly distributed in the lower frame, indicating a low Ca content, with similar size to that of 75-95% of the aluminosilicate content. There are also some points of C1 dispersed in the upper left zone with much smaller size and very calcium content. Those particles are likely to be calcite, anhydrite, calcium phosphate or other calcium-rich minerals derived solely from limestone, since concentration of calcium in raw sludge is low. The lower zone indicates that the minerals of cyclone ash are almost completely aluminosilicate and low in calcium, and the concentration of alkali metals seems independent of other elements in this common area for C1 and S1. What should be noted is that all particles contained Al and Si to some extent meaning any calcium in cyclone must have been bond with the aluminosilicate. XRD analysis was used to try to further demonstrate the reaction between calcium and aluminosilicates (See Supplementary Material), while there was no obviously new peak for CA samples which means that no crystal Ca-Si-Al mineral was generated or the crystal size was not large enough. But we cannot deny the conversion of calcium as it could form amorphous matter [23] and the analysis testified that CaO or $CaCO_3$ was reacted otherwise peaks of crystal with

223 calcium would have been detected. The formation of amorphous calcium can be attributed to the short resident time
224 for crystal growth when sludge passed through the furnace.

225 EDS statistics for fly ash is shown in Fig. 6(b), which was divided into two zones. It should be noticed that
226 the scale of axis Y is one fourth of Fig. 6(a), suggesting that the calcium-rich minerals in Fig. 6(a) were excluded
227 in the fly ash. This information further concluded that the second possibility, that calcium from limestone
228 directly formed those fine particles, does not hold. All S1 and most C1 points are distributed in the bottom zone,
229 where the sizes and distribution range are very similar with the lower zone in Fig. 6(a), mean that fly ash
230 (excluding submicron particle) of S1 as well as most that of C1 is aluminosilicate (mass fraction of 70-95%),
231 which was produced from fragment of raw sludge ash. There are only C1 points in the upper zone showing the
232 effect of limestone addition was proportional across all particles analysed. Some points in upper left are slightly
233 richer in Ca and aluminosilicate (total mass fraction of 76-83%) but poor alkali metals. Those particles came
234 from the fragments of agglomerated coarse particles described above. Other points in upper right are rich in
235 calcium and alkali metal but less Al and Si (total mass fraction of 50-80%). However, those samples were also
236 found to contain more phosphorous and sulphur which are higher volatility [30] . To sum up, the formation of
237 calcium-aluminosilicate by limestone enhanced the agglomeration of ash particles, then its fragment increased
238 to $PM_{2.5}$ and leading to more vaporization and condensation of semi-volatile elements [31] .

239

240 3.3 Distribution of heavy metals

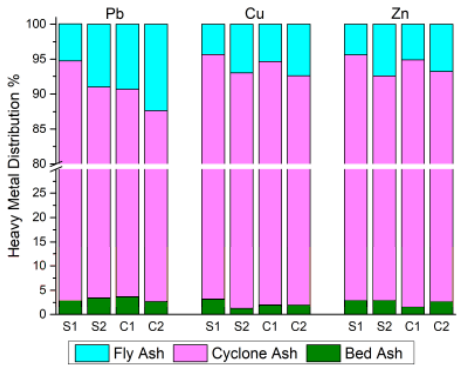

Fig. 7. Partitioning of heavy metals in different ash samples

The partitioning of heavy metals is shown in Fig. 7. The recovery rates of those three heavy metals were between 88% and 113%. The fly ash distribution rates of Pb ranged from 5.3% to 12.3%, and was highest among these three elements tested, while those of Zn and Cu are between 4.3% and 7.4% due to lower vaporisation temperature of Pb [32] . It is not desirable, but apparently that higher fuel feeding rate and limestone addition caused all heavy metals' partitions to increase in the fly ash. There might be some gaseous heavy metals adsorbed in drying bottle (with H_2SO_4 inside), but it was not detected by AAS, perhaps the concentrate was below the level of detection.

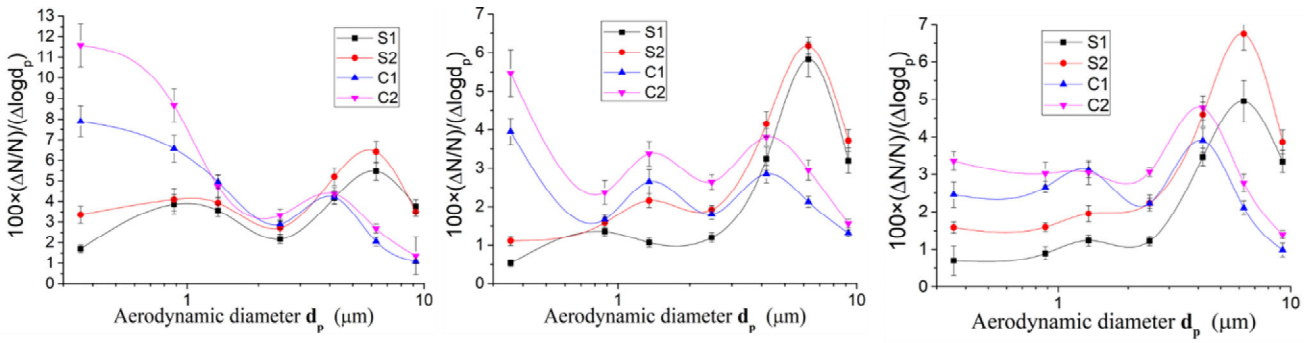

(a) Pb (b) Cu (c) Zn

Fig. 8. Heavy metal distribution in the particulate matter

Fig. 8 shows the distribution of three heavy metals in the PM, of which there are some common features for all elements reflecting the influences by different conditions as well as PM mass distribution. First of all, experiments conducted with the same feedstock and test conditions present, to some extent, similar trends with that of PM mass distribution curves in Fig. 4, where limestone addition affected the distribution more than fuel

feeding rate. As the limestone changed the partition of PM, it influenced the partition of heavy metals simultaneously [32] .

Secondly, the distributions of heavy metals in $PM_{2.5}$ and PM_1 reached a high level for the CA conditions. It has been previously demonstrated by extensive research that semi-volatile metals are more likely to accumulate in submicron particles [15] , but the partition of heavy metals in PM_1, especially for Pb, seems much greater for CA conditions, compared with SL conditions. Moreover, a higher fuel feeding rate also increased distributions of heavy metals in the $PM_{2.5}$ and PM_1.

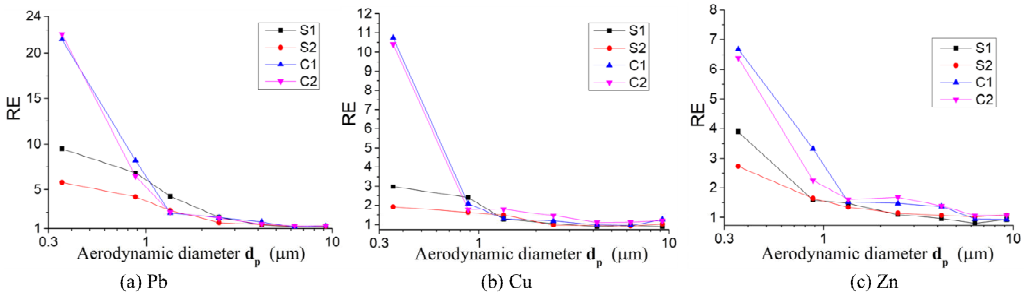

Fig. 9. Relative enrichment coefficient of heavy metals in the particulate matter.

To further reveal the relation between the partitioning of PM and heavy metals, and also to explain the effect of limestone addition, Fig. 9 presents the enrichment of heavy metals in the PM, where RE (Relative Enrichment Coefficient) increased with PM size decreasing. As RE is a relative coefficient for concentration, it focuses on whether and to what extent the element resides in a sample compared with the raw fuel. At the particle size range of 2.5-10μm, RE for each heavy metal and each condition is below 2, showing a little enrichment tendency resulted from increasing specific surface area. However, when the diameter is smaller than the inflection points of about 1μm, the RE values for most conditions rose sharply, especially for the CA conditions. Since the PM in this size range was generated from condensation and coagulation, those heavy metals also participated in this process and were present higher concentrations.

The common feature of each subplot in Fig. 8 is that limestone addition increased the concentration of heavy

metals in PM_1 and to reach those high concentrations, the vapor pressure for the gaseous heavy metals must have been high enough and there must be some interaction/influence between the limestone and vaporised metals. Previous work has studied how calcium stimulates the volatile of heavy metals during the combustion of the same sludge as that in this paper [23] . Combined with the analysis shown in Fig. 6, the alkali metals were also shown to volatilise from the fuel such that they can formed more ultra-fine particles [33] , which also helped enriched heavy metals in PM_1 by heterogeneous condensation.

As for heavy metal species in PM_1, Pb shows a higher concentration in submicron particles than Cu and Zn, because of its higher volatility in the furnace, which then tended to condense onto the fine particles with a larger specific surface area.

3.4 Mechanism and effect discussion

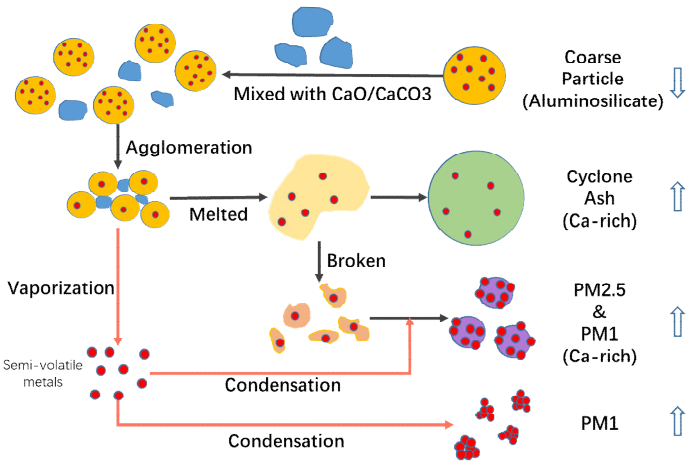

Fig. 10. Effect of limestone on PM and heavy metals

The effect of limestone on PM formation and heavy metal behaviours is coupled to the sludge combustion process, as Fig. 10 displays. After ignition, the sludge pellets are broken into pieces, some of which will become PM_{10} size particles. If limestone is present, then they collide with the CaO or $CaCO_3$ fragments and agglomerate and form eutectic mixtures. Simultaneously, the heavy metals and alkali metals are promoted to release in a gaseous form, rising their vapor pressure in the furnace.

293 The molten eutectic particles can then become cyclone ash with a high calcium content, since they are larger
294 enough to be captured by cyclone, however some may be broken into fragments and leave as fine particles.
295 These fine particles also provide a surface for vaporised heavy metals to condense. The remaining vaporized
296 semi-volatile metals end up resulting in more PM_1 as they condense into PM_1 and $PM_{2.5}$ particles.
297 Though the mineral of sludge in this paper was aluminosilicate, fuel containing other kinds of main mineral
298 may present a different behaviour. Bozaghian et al found increasing emissions of PM_1, containing KCl, during
299 co-combustion of straw and $CaCO_3$ [33] , whereas limestone addition, for desulfurization for combustion of
300 coal or sludge with a high sulfur content, reduced the emissions of PM_1 [18] . Moreover, different reactor types
301 (such as pulverized furnaces) and different operating conditions may also lead to different rates of PM and heavy
302 metal distribution. But the phenomenon found in this paper should be considered when determining whether or
303 not to blend limestone for in-furnace flue gas desulfurization during solid waste incineration, although it is a
304 popular method for SO_2 emission control.
305

306 # 4. Conclusion

307 This research investigated heavy metal and particulate matter emission characteristics during sludge
308 incineration in a fluidised bed furnace, where it was found that blending limestone with the sludge feedstock
309 significantly decreased the SO_2 in the flue gas, but the partitioning of fine particles (PM_1 and $PM_{2.5}$) and heavy
310 metals (lead, copper and zinc) in submicron was dramatically increased instead. The factor of fuel feeding rate
311 was also studied, showing that a higher feeding rate of fuel resulted in higher CO but lower NO_x emissions.
312 Additionally, PM emissions were a little greater because a higher local temperature and more inter-particle
313 collisions leading to greater fragmentation.
314 Based on SEM-EDS analysis and data statistics, the addition of limestone promoted the agglomeration and

fragmentation of ash particles simultaneously, leading to less PM_{10} but more $PM_{2.5}$ and cyclone ash. The addition of limestone increased the release of semi-volatile metals in the furnace, creating more PM_1 due to the "vaporization-condensation mechanism", and also provided more surface area for heavy metal condensation. As some heavy metals are also semi-volatile elements (Pb, Cu, Zn), calcium promoted their volatile in the furnace, and this is why their enrichments were enhanced in submicron particles.

In-furnace desulfurization of fluidised bed combustors by the addition of limestone is widely used in industry, but according to this research, more attention should be paid to the potential risk of stimulating higher PM and heavy metal emissions in some certain circumstances.

Acknowledgements

The authors would like to thank the financial supports by National Nature Science Foundation of China No. 51676040, Nature Science Foundation of Jiangsu Province No. BK20181281 and China Scholarship Council.

References

[1] Fytili D, Zabaniotou A. Utilization of sewage sludge in EU application of old and new methods-A review. Renew Sustain Energy Rev 2008;12:116–40.

[2] Gulyurtlu I, Lopes MH, Abelha P, Cabrita I, Oliveira JFS. The study of partitioning of heavy metals during fluidized bed combustion of sewage sludge and coal. J Energy Resour Technol Trans ASME 2006;128:104–10.

[3] Pudasainee D, Seo YC, Kim JH, Jang HN. Fate and behavior of selected heavy metals with mercury mass distribution in a fluidized bed sewage sludge incinerator. J Mater Cycles Waste Manag 2013;15:202–9.

[4] Yoo JI, Kim KH, Jang HN, Seo YC, Seok KS, Hong JH, et al. Emission characteristics of particulate matter and heavy metals from small incinerators and boilers. Atmos Environ 2002;36:5057–66.

[5] Tissari J, Sippula O, Torvela T, Lamberg H, Leskinen J, Karhunen T, et al. Zinc nanoparticle formation and physicochemical properties in wood combustion - Experiments with zinc-doped pellets in a small-scale boiler. Fuel 2015;143:404–13.

[6] Li Y, Man J, Fang Z, Zhao Y, Wang F, Li R. Formation and growth mechanisms of ultrafine particles in sludge incineration flue gas. Waste Dispos Sustain Energy 2019;1:143–50.

[7] Zhang P, Yu D, Luo G, Yao H. Temperature Effect on Central-Mode Particulate Matter Formation in Combustion of Coals with Different Mineral Compositions. Energy and Fuels 2015, 29:5245-52.

[8] Sun W, Liu X, Xu Y, Zhang Y, Chen D, Chen Z, et al. Effects of the modified kaolin sorbents on the reduction of ultrafine particulate matter (PM 0.2) emissions during pulverized coal combustion. Fuel 2018;215:153–60.

[9] Ninomiya Y, Zhang L, Sakano T, Kanaoka C, Masui M. Transformation of mineral and emission of particulate matters during co-combustion of coal with sewage sludge. Fuel 2004;83:751–64.

[10] Nigay PM, Nzihou A, White CE, Soboyejo WO. Accumulators for the Capture of Heavy Metals in Thermal Conversion Systems. J Environ Eng (United States) 2018;144:1–9.

[11] Han J, Xu M, Yao H, Furuuchi M, Sakano T, Kanchanapiya P, et al. Partition of heavy and alkali metals during sewage sludge incineration. Energy and Fuels 2006;20:583–90.

[12] Huang Q, Yu B, Qiu K, Zhou G, Wang S, Chi Y, et al. Effect of moisture on sewage sludge combustion temperature profile and heavy metal leaching. Dry Technol 2016;34:1810–9.

[13] Niu S, Chen M, Li Y, Lu T. Combustion characteristics of municipal sewage sludge with different initial moisture contents. J Therm Anal Calorim 2017;129:1189–99.

[14] Wang X, Huang Y, Liu C, Zhang S, Wang Y, Piao G. Dynamic volatilization behavior of Pb and Cd during fixed bed waste incineration: Effect of chlorine and calcium oxide. Fuel 2017;192:1–9.

[15] Xu Y, Liu X, Wang H, Zhang Y, Qi J, Xu M, Investigation of Simultaneously Reducing the Emission of Ultrafine

359 Particulate Matter and Heavy Metals by Adding Modified Attapulgite During Coal Combustion. Energy and Fuels
360 2019; 33(2):1518-26.
361 [16] Yao H, Naruse I. Control of trace metal emissions by sorbents during sewage sludge combustion. Proc Combust Inst
362 2005;30 II:3009–16.
363 [17] Zhang Y, Liu X, Xu Y, Sun W, Xu M. Investigation of reducing ultrafine particulate matter formation by adding
364 modified montmorillonite during coal combustion. Fuel Process Technol 2017;158:264–71.
365 [18] Chen J, Yao H, Zhang P, Xiao L, Luo G, Xu M. Control of PM1 by kaolin or limestone during O2/CO2 pulverized
366 coal combustion. Proc Combust Inst 2011;33:2837–43.
367 [19] Zheng W, Ma X, Tang Y, Ke C, Wu Z. Heavy Metal Control by Natural and Modified Limestone during Wood Sawdust
368 Combustion in a CO2/O2 Atmosphere. Energy and Fuels 2018;32:2630–7.
369 [20] Wang SJ, He PJ, Shao LM, Zhang H. Multifunctional effect of Al2O3, SiO2 and CaO on the volatilization of PbO
370 and PbCl2 during waste thermal treatment. Chemosphere 2016;161:242–50.
371 [21] Folgueras MB, Díaz RM, Xiberta J, Alonso M. Effect of inorganic matter on trace element behavior during
372 combustion of coal-sewage sludge blends. Energy and Fuels 2007;21:744–55.
373 [22] Lucie B, Zdeněk K. Effect of CaO on retention of S, Cl, Br, As, Mn, V, Cr, Ni, Cu, Zn, W and Pb in bottom ashes
374 from fluidized-bed coal combustion power station. J Environ Sci 2014;26:1429-36.
375 [23] Zha J, Huang Y, Xia W, Xia Z, Liu C, Dong L, et al. Effect of mineral reaction between calcium and aluminosilicate
376 on heavy metal behavior during sludge incineration. Fuel 2018;229:241–7.
377 [24] Allen D, Hayhurst AN. The effect of CaO on emissions of nitric oxide from a fluidised bed combustor. Fuel
378 2015;158:898–907.
379 [25] Ji X, Bie H, Zhang Y, Chen P, Fang W, Bie R. Release of K and Cl and Emissions of NOx and SO2 during Reed Black
380 Liquor Combustion in a Fluidized Bed. Energy and Fuels 2017;31:1631–7.

[26] Lopes MH, Abelha P, Lapa N, Oliveira JS, Cabrita I, Gulyurtlu I. The behaviour of ashes and heavy metals during the co-combustion of sewage sludges in a fluidised bed. Waste Manag 2003;23:859–70.

[27] Hernandez AB, Ferrasse JH, Chaurand P, Saveyn H, Borschneck D, Roche N. Mineralogy and leachability of gasified sewage sludge solid residues. J Hazard Mater 2011;191:219–27.

[28] Jiang X, Chen D, Ma Z, Yan J. Models for the combustion of single solid fuel particles in fluidized beds: A review. Renew Sustain Energy Rev 2017;68:410–31.

[29] Zhang T, Liu Z, Huang X, Sun Q, Liu C, Li J, et al. Computer-controlled scanning electron microscopy investigation on ash formation characteristics of a calcium-rich coal under O2/CO2 environments. Energy and Fuels 2017;31:319–27.

[30] Ke C, Ma X, Tang Y, Tang F, Zheng W. Effects of natural and modified calcium-based sorbents on heavy metals of food waste under oxy-fuel combustion. Bioresour Technol 2019;271:251–7.

[31] Calvo AI, Tarelho LAC, Teixeira ER, Alves C, Nunes T, Duarte M, et al. Particulate emissions from the co-combustion of forest biomass and sewage sludge in a bubbling fluidised bed reactor. Fuel Process Technol 2013;114:58–68.

[32] Linak WP, Wendt JOL. Toxic metal emissions from incineration: Mechanisms and control. Prog Energy Combust Sci 1993;19:145–85.

[33] Bozaghian M, Rebbling A, Larsson SH, Thyrel M, Xiong S, Skoglund N. Combustion characteristics of straw stored with CaCO3 in bubbling fluidized bed using quartz and olivine as bed materials. Appl Energy 2018;212:1400–8.